JPL D-101765

MSPI

Multiangle SpectroPolarimetric Imager

AirMSPI Data Quality Statement: SPEX-PR Campaign

David J. Diner (PI), Michael J. Garay, Carol J. Bruegge, Felix C. Seidel, Michael A. Bull, Veljko M. Jovanovic, Irina N. Tkatcheva, Brian E. Rheingans, Gerard van Harten, Feng Xu, Abigail M. Nastan
Corresponding Author: Michael.J.Garay@jpl.nasa.gov

JPL

Jet Propulsion Laboratory
California Institute of Technology

20 April 2018

Distributed by the Atmospheric Science Data Center
http://eosweb.larc.nasa.gov

Campaign	
Name	SPEX engineering flights + Porter Ranch gas leak overflights (SPEX-PR)
Dates	2 February - 9 February 2016
Locations	California and Pacific Ocean
ER-2 remote sensing instruments	AirMSPI, AVIRIS, SPEX
Publications	http://doi.org/10.5194/amt-9-2877-2016 http://doi.org/10.1002/2017JD026776

AirMSPI Overview of Data Calibration and Processing to Level 1 B2	
Data (Ellipsoid projected)	http://doi.org/10.5067/AIRCRAFT/AIRMSPI/SPEX-PR/RADIANCE/ELLIPSOID_v006
Data (Terrain projected)	http://doi.org/10.5067/AIRCRAFT/AIRMSPI/SPEX-PR/RADIANCE/TERRAIN_v006
Data Delivery Version	V006
PGE Software Version	10.2.3
Lab. Cal. Software Version	6.7
Radiometric Calibration	30 March 2016
Polarimetric Calibration	15 April 2016
Vicarious Calibration	5 July 2016
Lin. Cal. File	airmspi_lincal_20110921_v6.7.dat
Rad. Cal. File	airmspi_radcal_lab20160330v6.7_vc20160705_update20170418.dat
Pol. Cal. File	airmspi_polcal_20160415_v6.7.dat

Distributed by the Atmospheric Science Data Center
http://eosweb.larc.nasa.gov

JPL D-101765

Airborne Multiangle SpectroPolarimetric Imager (AirMSPI)

AirMSPI Data Quality Statement: SPEX-PR Campaign

APPROVALS:

David J. Diner

AirMSPI Principal Investigator

© 2018 California Institute of Technology. Government sponsorship acknowledged.

Approval signatures are on file with the AirMSPI Project.
To determine the latest released version of this document, consult the AirMSPI web site (http://airbornescience.jpl.nasa.gov/instruments/airmspi/).

Jet Propulsion Laboratory
California Institute of Technology

Distributed by the Atmospheric Science Data Center
http://eosweb.larc.nasa.gov

Document Change Log

Revision	Date	Affected Portions and Description
	20 April 2018	Original release

Which Product Versions Does this Document Cover?

Product Filename Prefix	Version Number in Filename	Brief Description
AirMSPI_ER2_GRP_ELLIPSOID	V006	L1B2 Ellipsoid-Projected Georectified Radiance and Polarization Data
AirMSPI_ER2_GRP_TERRAIN	V006	L1B2 Terrain-Projected Georectified Radiance and Polarization Data

Distributed by the Atmospheric Science Data Center
http://eosweb.larc.nasa.gov

TABLE OF CONTENTS

Distributed by the Atmospheric Science Data Center
http://eosweb.larc.nasa.gov

1 INTRODUCTION

1.1 AirMSPI L1B2 Products

The Airborne Multiangle SpectroPolarimetric Imager (AirMSPI) Level 1B2 products contain radiometric and polarimetric observations of clouds, aerosols, and the surface of the Earth made from the National Aeronautics and Space Administration's (NASA) ER-2 high altitude research aircraft. The AirMSPI instrument acquires data using one of two possible modes, step-and-stare and sweep. Step-and-stare data are gridded with 10 m spatial sampling, with one file provided for each view angle. Sweep data are gridded with 25 m spatial sampling. Files are distributed in HDF-EOS-5 format.

The purpose of this document is to describe the data quality of the AirMSPI L1B2 products specifically for the SPEX engineering flights + Porter Ranch gas leak overflights (SPEX-PR) field campaign, which took place in California and over the Pacific Ocean in February 2016.

1.2 AirMSPI Data Processing and Distribution

The MISR Science Computing Facility (SCF) at the Jet Propulsion Laboratory (JPL) supports the development of AirMSPI science algorithms and software, instrument calibration and performance assessment, and also provides quality assessment and data validation services with respect to AirMSPI Science Data Processing (SDP). The MISR SCF is used to perform the standard processing of the AirMSPI data. After AirMSPI data processing is complete, the standard output products are archived and made available to users via the Langley Research Center (LaRC) Atmospheric Science Data Center (ASDC) client services. See https://eosweb.larc.nasa.gov/project/airmspi/airmspi_table.

1.3 Controlling Documents

1) Multiangle Spectropolarimetric Imager (MSPI) Algorithm Theoretical Basis Document Rev. B Draft, November 2009 (or latest version).

1.4 Related Documents

1) AirMSPI Data Product Specification for the AirMSPI Level 1B2 Products (V006), JPL D-100825, Rev. C, September 2017 (or latest version).

Distributed by the Atmospheric Science Data Center
http://eosweb.larc.nasa.gov

2 RADIOMETRIC CALIBRATION

2.1 Laboratory Calibration

Laboratory radiometric calibration of the AirMSPI instrument (Diner et al., 2013a) was conducted on 30 March 2016 (after the SPEX-PR field campaign) by observing the output port of a 1.65 m integrating sphere. The sphere illuminates the entire field of view of the instrument. Data were collected at multiple light levels and the sphere output was monitored with an Analytical Spectral Devices (ASD) FieldSpec Pro spectrometer in order to generate a digital number (DN) vs. radiance regression for each pixel. The AirMSPI line arrays have 1536 pixels in each channel. Offset levels are determined from observations in 100 pixels at the end of each array that are shielded from illumination; hence only 1436 pixels in each line collect image data. After correction for non-linearity (lincal), gain factors are computed on a per-pixel basis for each channel. The 13 spectral channels of the instrument measure incident radiance at wavelengths close to 355, 380, 445, 470, 555, 660, 865, and 935 nm (8 bands). In keeping with Stokes parameter nomenclature, the polarization channels report I, Q, and U, where I is the total measured radiance. The Stokes parameters Q (excess of horizontally over vertically polarized light) and U (excess of 45° over 135° polarized light) are reported for the bands at 470, 660, and 865 nm. Note that the AirMSPI instrument does not have a separate radiance-only channel at 470 nm. The radiance reported in the AirMSPI data products for this channel is obtained independently from the demodulated 470Q and 470U channel data and is the mean of the values derived from these two channels. Thus, although the AirMSPI instrument itself only has 13 spectral channels, 14 spectral channels are reported in the AirMSPI L1B2 products.

Although gain factors are derived on a per-pixel basis, residual striping can appear in Earth images, particularly in the UV bands. It is believed that this striping is the result of out-of-band spectral leakage due to physical imperfections in the focal plane filter.

2.2 Vicarious Calibration

On 05 July 2016, AirMSPI overflew the parking lot at Hangar 703, Armstrong Research Flight Center. Data were taken both from the air, and by a team on the ground. For the latter, both the reflectance of the parking lot, surface pressure, and aerosol loading measurements were made. Instrumentation included an Analytic Spectral Devices (ASD) field spectrometer and a Microtops sunphotometer. These data were used as input to the Markov radiative transfer code, which produced top-of-atmosphere spectral radiances. The Markov code is a vector code, tracing polarization components through the atmosphere. This vicarious calibration of AirMSPI had band-dependent agreement with the laboratory calibration. Differences ranged from 15% in the UV to 1% agreement in the mid-visible. The radiometric calibration of AirMSPI was set using this vicarious calibration. It is believed to have a higher accuracy than the laboratory calibration, due to the low UV light levels used to calibrate in the laboratory.

Distributed by the Atmospheric Science Data Center
http://eosweb.larc.nasa.gov

2.3 Calibration Traceability

AirMSPI calibrations are traceable to *Système international* (SI) Units, via National Institute of Standards and Technology (NIST) standards. For laboratory calibrations, this is through a reference 20.32 cm (8 inch) integrating sphere, calibrated annually by the vendor, Gooch & Housego (http://goochandhousego.com/). For vicarious calibrations, this is through a Spectralon reflectance standard located at the vicarious calibration site.

2.4 Radiometric Data Quality Indicators

Following the practice adopted by the Multi-angle Imaging SpectroRadiometer (MISR) project, each AirMSPI pixel is assigned a Radiometric Data Quality Indicator (RDQI). The RDQI definitions are as follows:

RDQI = 0: No radiometric issues are identified.

RDQI = 1: The radiometric quality does not meet an identified threshold but is deemed usable for scientific analysis purposes.

RDQI = 2: The radiometric quality does not meet a secondary threshold and the data from this pixel should not be used for scientific analysis purposes.

RDQI = 3: The quality of the pixel is scientifically and cosmetically unusable. In addition, the shielded pixels at the end of each line array are marked with RDQI of 3.

During laboratory calibration, a "gain" is computed from the slope of camera output DN to total-band incident radiance, *I*. It is observed that pixels with a large out-of-band leakage have a larger uncertainty in this gain, in that it is observed to vary with the spectrum of the incident light. A data quality indicator can thus be computed based on the change in gain with different illumination sources. Specifically, we take the ratio of the gain computed with an incandescent lamp to the gain computed from adding a UV plasma lamp. Pixels for which this gain ratio is between 0.95 and 1.05 are assigned an RDQI value of 0 indicating that out-of-band light is a small contributor to the measured radiance. Pixels for which the gain ratio is outside of this range, but between 0.90 and 1.10 are assigned an RDQI value of 1. Pixels with gain ratios outside both these ranges, but between 0.80 and 1.20 are assigned an RDQI value of 2. All other pixels are assigned an RDQI value of 3. Note that for the 470I channel, for which the reported radiance is the mean of the demodulated 470Q and 470U channel data, the RDQI is likewise calculated as the mean (rounded to the nearest integer) of the RDQI values for these two channels. The observed out-of-band leakage is believed to be the cause of striping in the images, which is particularly noticeable in the UV bands.

Occasionally, scene elements (e.g., deep clouds or sunglint) are so bright as to cause saturation in some pixels. Future versions of the AirMSPI product may flag these situations, but this has not been done for the current version of the publicly available data. Isolated pixels that experienced saturation in one or more channels are readily identifiable in the imagery due to their anomalous appearance. In some scenes, saturation affected a significant portion of the imagery at a particular

Distributed by the Atmospheric Science Data Center
http://eosweb.larc.nasa.gov

view angle, and release of those data is delayed pending implementation of the saturation flag. In other cases, users may notice that the files corresponding to the aftmost angles are shorter than normal, or missing. This can occur, for instance, when the step-and-stare observing sequence was terminated early by the ER-2 pilot.

As described above, for the 470 nm radiance channel, information from two polarimetric channels – a channel measuring *I* and *Q*, and a channel measuring *I* and *U* – is used to generate the data reported in the L1B2 product. The RDQI values reported for the 470 nm *I* radiance channel represent the maximum of the values reported separately for these two channels. For the 660 and 865 nm bands, three channels are used to generate the data reported in the L1B2 product: a channel measuring *I* only, a channel measuring *I* and *Q*, and a channel measuring *I* and *U*. The RDQI values reported for these channels represent the values in the non-polarimetric *I* channel, and are typically 0.

Pixels marked with RDQI = 0 are expected to have an absolute radiometric uncertainty of ~5% (1σ). This radiometric uncertainty is attributed to the vicarious calibration methodology, which sets the absolute radiometric scale. The laboratory calibration is used to establish the relative-pixel response, also known as "flat-fielding". Comparisons of vicarious calibrations before (10 November 2015) and after (5 July 2016) the campaign suggest that the sensor remained stable during the campaign.

3 SPECTRAL CALIBRATION

Determination of the detailed spectral response function (SRF) of each AirMSPI channel has been made based on the laboratory calibration of 9 December 2013. A monochromator was used for this purpose. The SRF is equal to the camera response to monochromatic light normalized by a silicon diode response. The monochromator provided wavelength scans from 300 to 2500 nm. Two sources were used in separate spectral scans of all channels — a Luxim Light Emitting Plasma lamp for ultraviolet-blue, and a quartz-halogen lamp for the remaining visible and near-infrared channels. The results of this calibration are shown in Table 1 and Figure 2.

In the current product release (V006), center wavelengths, effective (equivalent square-band) bandwidths, and effective (equivalent square-band) transmittances are calculated by applying the moments method of Palmer (1984) to the normalized spectral response of each band over the range 300-1100 nm. Solar irradiances are weighted by the total-band spectral response. The Wehrli (1985) extraterrestrial solar spectrum was used for this purpose. These values are provided in Table 1 below, and represent the total-band response. Again, the values reported for the 470I channel represent the mean of the demodulated 470Q and 470U channel values.

In general, radiometric response at wavelengths far from the "in-band" spectral region is estimated at $< 10^{-4}$ of the peak response, though as noted above, a larger amount of out-of-band leakage is present in a small subset of pixels in the UV bands, leading to striping in a portion of the UV images. Currently uncorrected striping in the 355 and 380 nm bands is attributed to filter blemishes that create a scene-dependent scattered light response.

Distributed by the Atmospheric Science Data Center
http://eosweb.larc.nasa.gov

Table 1 – Total-band effective center wavelength, bandwidth and transmittance, and total-band weighted solar irradiance E_0 [W m^{-2} nm^{-1}] at 1 AU

Channel Name	Center Wavelength (nm)	Effective Bandwidth (nm)	Effective Transmittance	Solar Irradiance (W m^{-2} nm^{-1})
355I	355.1	47.7	0.609	1.002
380I	377.2	40.4	0.750	1.079
445I	443.3	46.0	0.799	1.861
470I	469.1	45.5	0.824	2.000
470Q	469.4	45.0	0.837	1.999
470U	468.8	46.0	0.815	2.000
555I	553.5	38.6	0.758	1.857
660I	659.2	45.2	0.835	1.555
660Q	659.1	43.8	0.881	1.556
660U	659.1	48.2	0.798	1.556
865I	863.3	43.5	0.829	0.976
865Q	863.7	45.6	0.810	0.976
865U	864.1	48.5	0.753	0.975
935I	931.3	53.2	0.809	0.823

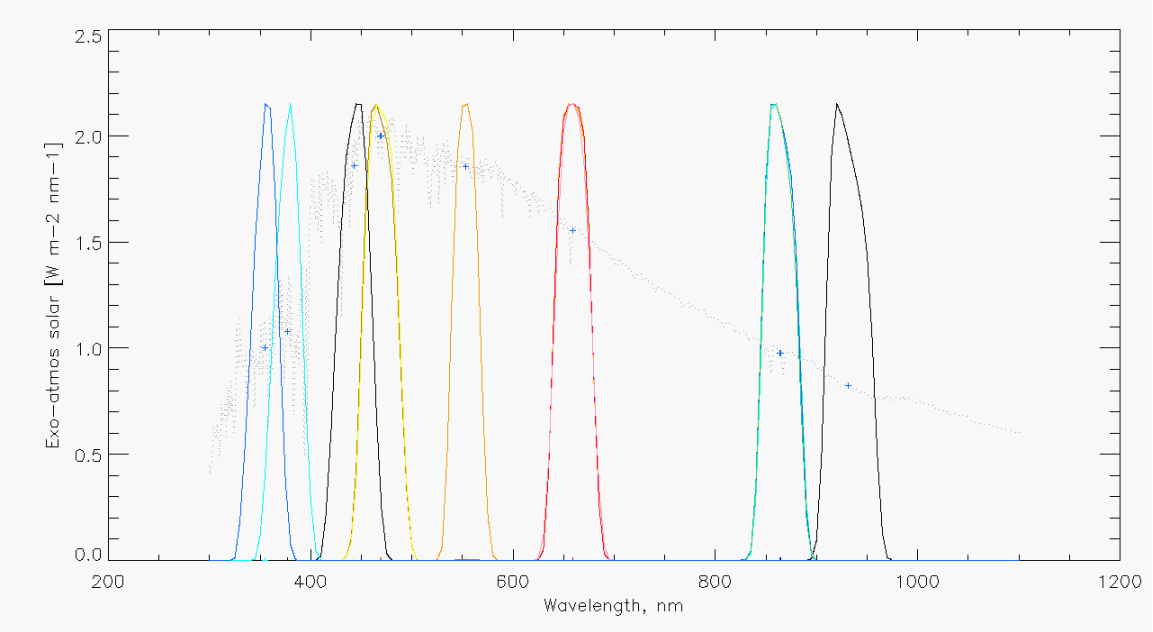

Figure 2. AirMSPI spectral response functions (SRF) shown in colored lines with the Wehrli (1985) exoatmospheric solar irradiance values shown in the faint, gray, dotted line. E0 values at 1 AU are indicated by the "+" symbol.

Distributed by the Atmospheric Science Data Center
http://eosweb.larc.nasa.gov

4 POLARIMETRIC CALIBRATION

AirMSPI uses a time-varying retardance in the optical path to modulate the orientation of the linearly polarized component of the incoming light, described by the Stokes components Q (excess of horizontally over vertically polarized light) and U (excess of 45º over 135º polarized light) (Diner et al., 2007, 2010; Mahler et al., 2011). As a result, the ratios of these parameters to the radiance I, given by $q = Q/I$ and $u = U/I$ are to first order insensitive to the absolute radiometric calibration of a given pixel because both the numerator and denominator are determined from signals acquired by the same detector element. The degree of linear polarization (DOLP) and angle of linear polarization (AOLP) derived from these ratios, equal to $\sqrt{q^2 + u^2}$ and $0.5\tan^{-1}(u/q)$, respectively, are likewise insensitive to absolute radiometric calibration, based on similar considerations. To compensate for instrumental polarization aberrations (e.g., mirror diattenuation, imperfect retardance), a set of 10 polarimetric calibration coefficients is established for every pixel (Diner et al., 2010).

Two specialized pieces of equipment exist for verifying and controlling the performance of the polarimetric measurement approach during in-flight operations of AirMSPI. The first is an optical probe, which continuously sends a beam of light through the photoelastic modulators (PEMs) to monitor their retardances and phases. The information from the probe shows how far the PEM retardances and phases are from their desired values. A feedback control system within the instrument then adjusts the PEM parameters to drive the error signals to zero. Test data demonstrated the ability to control the PEM retardance and phase parameters to within a fraction of 1 mrad, keeping contributions to the overall DOLP uncertainty budget at <0.001. The second polarization monitoring system is an external polarization validator, which consists of nine light-emitting diodes (LEDs), three each at the AirMSPI polarimetric bands, that illuminate a plastic diffuser. In front of the diffuser, sheet polarizers are placed in different orientations. The validator is viewed before and after every multiangle observation of an Earth scene. Information from the validator system is used to derive instrument dark current and evaluate the stability of the DOLP measurements.

Results from a ground-based version of the instrument, GroundMSPI (Diner et al., 2012), show systematic DOLP uncertainties (excluding the effects of random noise), determined as the root-mean-square residual in DOLP as a polarizer is rotated in front of the camera, of ±0.003 or better. Results for AirMSPI, using the rotating polarizer methodology described in Diner et al. (2010), show similar residuals.

5 GEORECTIFICATION AND CO-REGISTRATION

As a part of the ground data processing, AirMSPI data from all spectral bands and all viewing angles are georectified and co-registered to a common Earth-based, Universal Transverse Mercator (UTM) projection grid. Distortions that can be associated with AirMSPI's type of pushbroom remote sensing imaging are taken into account by properly defining instantaneous pixel projection rays using ancillary data such as estimates of camera internal viewing geometry and ER-2 navigation data, which provide dynamic measures of the platform altitude and attitude variations. There are two types of AirMSPI georectified data products: 1) terrain projected and 2) ellipsoid projected. Terrain-projected data use a digital elevation model (DEM) for the projection surface

Distributed by the Atmospheric Science Data Center
http://eosweb.larc.nasa.gov

so that cloud-free imagery is truly orthorectified with reference to that surface. Ellipsoid-projected data use the World Geodetic System 1984 (WGS84) Earth reference ellipsoid for the projection surface. One purpose of the ellipsoid projection is to provide input to stereoscopic height retrievals for predominantly cloudy imagery. Automatic stereoscopic retrieval software is currently in development.

Factors affecting geospatial accuracy of AirMSPI products include: 1) relative band-to-band co-registration within a single viewing angle, 2) multi-angle co-registration, and 3) absolute georectification. The uncertainty depends on the magnitude of the errors in the supplied ancillary data and errors in the projection surface defined by the DEM. In the case of the SPEX-PR campaign, the United States Geological Survey (USGS)-provided National Elevation Dataset (NED) with 10 m horizontal posting and 2.44 m rms error in elevation is used. Errors in the ancillary data defining viewing geometry are handled as static and dynamic pointing errors in order to characterize them using available ground control points (GCPs) in a procedure based on simultaneous bundle adjustment (Jovanovic et al., 2012). For targets where there is an optimum number of GCPs available, both static and dynamic pointing errors are recovered simultaneously prior to georectification and co-registration. These data are denoted as having full geometric calibration "directly" applied with expected co-registration and georectification uncertainty of around 15 m rms across all viewing angles and all bands. For other targets, (i.e., those without available GCPs, which are mostly fully ocean or cloudy imagery), an estimate of static pointing errors made on separate flight lines within the same campaign is utilized. These products are denoted as having geometric calibration "indirectly" applied with a current estimate of georectification and co-registration uncertainty of less than one hundred meters. The type of geometric calibration is recorded in the file metadata list under the field name "Geolocation stage". Analysis and implementation efforts are still in progress with an objective to fully optimize the camera viewing model so that uncertainties of indirectly calibrated data are minimized.

Band-to-band relative co-registration uncertainty within the same viewing angle is well within 10 m, which is the pixel size of the map projection grid in the step-and-stare terrain-projected data. In the case of ellipsoid-projected data there will be some offsets in the relative band-to-band registration due to the parallax caused by the true height of the viewing surface and physical band separation in the focal plane. Additionally, slight errors in registration can cause a slight displacement (on the order of a degree or two) of polarimetric features such as the backscatter glory from their expected location.

Occasional gaps of isolated lines in AirMSPI pushbroom imagery are present in an extremely small number of scenes. These are due to changes in the ER-2 pitch attitude that occurred too abruptly (e.g., as the result of turbulence) to either: 1) be captured accurately in the ER-2 navigation data, and/or 2) cause occasional gaps in the imagery created in the pushbroom fashion.

Distributed by the Atmospheric Science Data Center
http://eosweb.larc.nasa.gov

6 INCIDENTAL DATA QUALITY ISSUES

On February 2, sun glint was observed over the Pacific Ocean. This specular reflection of sunlight off the ocean is bright, sometimes causing the detector to saturate, and highly polarized. The following sun glint images contain saturated pixels, causing NaN pixel values in the HDF files, as well as black pixels in the JPG quicklooks:

AirMSPI_ER2_GRP_ELLIPSOID_20160202_193441Z_CA-SouthGate_SWPF_F01_V006
AirMSPI_ER2_GRP_TERRAIN_20160202_193441Z_CA-SouthGate_SWPF_F01_V006
AirMSPI_ER2_GRP_ELLIPSOID_20160202_193600Z_NorthPacificOcean-34N118W_556F_F01_V006
AirMSPI_ER2_GRP_ELLIPSOID_20160202_193629Z_NorthPacificOcean-34N118W_492F_F01_V006
AirMSPI_ER2_GRP_ELLIPSOID_20160202_193658Z_NorthPacificOcean-34N118W_409F_F01_V006
AirMSPI_ER2_GRP_ELLIPSOID_20160202_194159Z_NorthPacificOcean-33N118W_SWPF_F01_V006
AirMSPI_ER2_GRP_ELLIPSOID_20160202_195345Z_NorthPacificOcean-33N118W_SWPA_F01_V006
AirMSPI_ER2_GRP_ELLIPSOID_20160202_195450Z_NorthPacificOcean-33N118W_SWPF_F01_V006
AirMSPI_ER2_GRP_TERRAIN_20160202_195450Z_NorthPacificOcean-33N118W_SWPF_F01_V006
AirMSPI_ER2_GRP_ELLIPSOID_20160202_195954Z_CA-LosAngeles_409A_F01_V006
AirMSPI_ER2_GRP_TERRAIN_20160202_195954Z_CA-LosAngeles_409A_F01_V006
AirMSPI_ER2_GRP_ELLIPSOID_20160202_200022Z_CA-LosAngeles_492A_F01_V006
AirMSPI_ER2_GRP_TERRAIN_20160202_200022Z_CA-LosAngeles_492A_F01_V006

February 9 was dedicated to overflying a methane gas leak in Porter Ranch, Los Angeles. For this purpose, the plane flew at a low altitude (700-5000 ft as opposed to the regular 65,000 ft) and conducted many rapid attitude changes. This causes image blurring, band coregristration imperfections, and gaps in the imagery during the following runs:

203347Z_CA-Castaic
203454Z_CA-SantaClarita
203600Z_CA-LosAngelesCounty
203814Z_CA-LosAngeles
203921Z_CA-SimiValley
210146Z_CA-SantaClarita
211413Z_CA-Castaic
211520Z_CA-Castaic
211841Z_CA-LosAngeles
211948Z_CA-LosAngeles
212731Z_GulfOfMexico-25N85W
213331Z_CA-LosAngeles
214112Z_CA-Castaic

Distributed by the Atmospheric Science Data Center
http://eosweb.larc.nasa.gov

7 REFERENCES

Diner, D.J., A. Davis, B. Hancock, G. Gutt, R.A. Chipman, and B. Cairns (2007). Dual photoelastic modulator-based polarimetric imaging concept for aerosol remote sensing. *Appl. Opt.* **46**, 8428-8445.

Diner, D.J., A. Davis, B. Hancock, S. Geier, B. Rheingans, V. Jovanovic, M. Bull, D.M. Rider, R.A. Chipman, A. Mahler, and S.C. McClain (2010). First results from a dual photoelastic modulator-based polarimetric camera. *Appl. Opt.* **49**, 2929-2946.

Diner, D.J., F. Xu, J.V. Martonchik, B.E. Rheingans, S. Geier, V.M. Jovanovic, A. Davis, R.A. Chipman, and S.C. and McClain (2012). Exploration of a polarized surface bidirectional reflectance model using the Ground-based Multiangle SpectroPolarimetric Imager. *Atmosphere* **3**, 591-619.

Diner, D.J., F. Xu, M.J. Garay, J.V. Martonchik, B.E. Rheingans, S. Geier, A. Davis, B.R. Hancock, V.M. Jovanovic, M.A. Bull, K. Capraro, R.A. Chipman, and S.C. McClain (2013a). The Airborne Multiangle SpectroPolarimetric Imager (AirMSPI): a new tool for aerosol and cloud remote sensing. *Atmos. Meas. Tech*. **6**, 2007-2025.

Diner, D.J., M.J. Garay, O.V. Kalashnikova, B.E. Rheingans, S. Geier, M.A. Bull, V.M. Jovanovic, F. Xu, C.J. Bruegge, A. Davis, K. Crabtree, and R.A. Chipman (2013b). Airborne Multiangle SpectroPolarmetric Imager (AirMSPI) observations over California during NASA's Polarimeter Definition Experiment (PODEX). *SPIE Proc*. **8873**, 88730B-2.

Jovanovic, V.M., M. Bull, D.J. Diner, S. Geier, and B. Rheingans (2012). Automated data production for a novel Airborne Multiangle SpectroPolarimetric Imager (AirMSPI). *Int. Arch. Photogramm. Remote Sens. Spatial Inf. Sci.*, **XXXIX-B1**, 33-38.

Mahler, A., D.J. Diner, and R.A. Chipman (2011). Analysis of static and time-varying polarization errors in the multiangle spectropolarimetric imager. *Appl. Opt.* **50**, 2080-2087.

Palmer, J.M. (1984). Effective bandwidths for LANDSAT-4 and LANDSAT-D' Multispectral Scanner and Thematic Mapper subsystems. *IEEE Trans. Geosci. Rem. Sens.* **GE-22**, 336-338.

Wehrli, C. (1985). "Extraterrestrial Solar Spectrum", Publication no. 615, Physikalisch Meteorologisches Observatorium + World Radiation Center (PMO/WRC) Davos Dorf, Switzerland, July 1985.

Distributed by the Atmospheric Science Data Center
http://eosweb.larc.nasa.gov

8 APPENDIX

Acronym List:

AirMSPI	Airborne Multiangle SpectroPolarimetric Imager
AOLP	Angle of Linear Polarization
ASD	Analytical Spectral Devices
ASDC	Atmospheric Science Data Center
AVIRIS	Airborne Visible/Infrared Imaging Spectrometer
AU	Astronomical Unit
DEM	Digital Elevation Model
DN	Digital Number
DOLP	Degree of Linear Polarization
EOS	Earth Observing System
GCP	Ground Control Point
HDF-EOS	Hierarchical Data Format for EOS
JPL	Jet Propulsion Laboratory
LaRC	Langley Research Center (NASA)
LED	Light-emitting diode
MISR	Multi-angle Imaging SpectroRadiometer
NASA	National Aeronautics and Space Administration
NED	National Elevation Dataset
NIST	National Institute of Standards and Technology
PEM	Photoelastic modulator
RDQI	Radiometric Data Quality Indicator
SCF	Science Computing Facility
SDP	Science Data Processing
SPEX	Spectropolarimeter for Planetary EXploration
SPEX-PR	SPEX engineering flights + Porter Ranch gas leak overflights
SI	*Système international*
SRF	Spectral Response Function
USGS	United States Geological Survey
UTM	Universal Transverse Mercator
UV	Ultraviolet
WGS84	World Geodetic System 1984

Distributed by the Atmospheric Science Data Center
http://eosweb.larc.nasa.gov

© 2013, 2014, 2015, 2016, 2017, 2018 California Institute of Technology. Government sponsorship acknowledged.

Distributed by the Atmospheric Science Data Center
http://eosweb.larc.nasa.gov